

Leakage Inductance Estimation of Toroidal Common-mode Choke from Perspective of Analogy between Reluctances and Capacitances

Ren Ren¹, Zhou Dong¹, Bo Liu³, Fred Wang^{1,2}

¹Min H. Kao Department of Electrical Engineering & Computer Science,
The University of Tennessee, Knoxville, TN, USA

²Oak Ridge National Laboratory, Knoxville, TN, USA

³United Technologies Research Center, CT, USA

rren3@vols.utk.edu

Abstract— To reduce the volume and weight of differential-mode (DM) inductors, the leakage inductance of a toroidal common-mode (CM) choke is often used as partial DM inductance. However, the accurate prediction of the leakage inductance of CM chokes through an analytical model is difficult, making the determination of remaining DM inductance difficult. This paper proposes a modeling method with the analogy between reluctances (or magnetic fields) and capacitances (or capacitive fields). The proposed method is verified by the leakage inductance comparison between the proposed model and simulation results for two CM cores with different turns numbers and wire gauges, and it demonstrated the proposed model can achieve the errors within 15% compared with simulation results for all cases.

Keywords—Leakage inductance, toroidal common mode choke, analogy, reluctance, capacitance

I. INTRODUCTION

Leakage inductance evaluation is important in the design of toroidal CM inductors. First, the accurate calculation of leakage inductance can avoid over-design or under-design of the individual DM inductance. Second, the DM flux induced core loss estimation in CM cores also highly depends on the accurate leakage inductance calculation.

By constructing an equivalent symmetrical geometry about the z-axis plane for toroidal cores, Ref. [1] developed a set of self and mutual impedance formulae directly from Maxwell's equations for coils on ferromagnetic cores in 2-D dimension. Although the model in [1] achieves an ultimate accuracy equivalent to a 2-D simulation with a FEM software, no closed-form solution is provided for simple use. Either Bessel functions or numerical method must be used to solve the equations with integrals, making it difficult to use in practical design. Paper [2] further simplified the impedance derivation of toroidal structures with 1-D dimension assumption (magnetic fields only change with the thickness of windings), and it is very effective for toroidal transformers with the bifilar windings or no air gap structures to minimize the leakage flux in the air. However, it is not a common practice in the CM inductor design for EMI application, and separate winding structures are more popular due to the usage of leakage inductance as the DM inductance.

To obtain a more applicable model, Nave [3] proposed a leakage inductance model based on his finding that the magnetic fields of rod core and the leakage flux of toroidal CM core are quite similar. Then the leakage inductance model of toroidal CM cores was derived with the existing rod core model [3]. However, the error of Nave's model is up to 30%~40% when the winding angle becomes larger with the increase of turns number. Heldwein [4] improved Nave's model by amending the effective leakage flux path length, but it only increases accuracy when the winding angle is smaller than 30° compared with Nave's model.

Zhou [5] developed a highly accurate model with Artificial Neural Network fitting of FEM simulation results by sweeping the selected input variables, achieving only 2.4 % error. Nonetheless, the proposed method needs much effort to obtain the training data with FEM simulations, and for different cores, no unified model can be directly applied and the fitting coefficients currently are only effective for one specific core.

Starting from a new perspective of the analogy between reluctances and capacitances, the proposed model, providing a closed-form equation, can achieve relatively high accuracy for toroidal cores and arbitrary turns numbers (winding angles).

II. ROD CORE INDUCTANCE DERIVATION WITH ANALOGY OF RELUCTANCE AND CAPACITANCE

In this section, Nave's idea of using a rod core inductance model to calculate the leakage inductance of CM cores is still assumed correct, but the adopted rod core inductance model will be based on the conventional inductance calculation equation with equivalent DM permeability and effective path length of the leakage flux, which is not accurate enough.

In case the error of the leakage inductance is caused by the inaccuracy of the rod core inductance model in [3], this paper adopts Payne's model [6], having a maximum 1.5% error compared with measuring results, to improve the accuracy of the leakage inductance prediction. Payne's derivation of the rod core inductance provides a new perspective from the analogy between reluctances and capacitances. The idea is to obtain rod core inductance

through the derivation of inductance ratio w/o the ferrite rod core, expressed as

$$L_f = L_{air} (L_f / L_{air}) = \frac{R_{in_air} + R_{out_air}}{R_{in_f} + R_{out_f}} L_{air} \quad (1)$$

$$= \frac{R_{in_air} / R_{out_air} + 1}{(R_{in_air} / \mu_f) / R_{out_air} + 1} L_{air}$$

where L_{air} is the air core inductance and L_f is the inductance with insertion of the rod ferrite core, R_{in_f} and R_{in_air} are the reluctance inside windings w/o the rod ferrite core, R_{out_f} and R_{out_air} are the reluctance outside winding w/o the rod ferrite core, and μ_f is the permeability of the ferrite core.

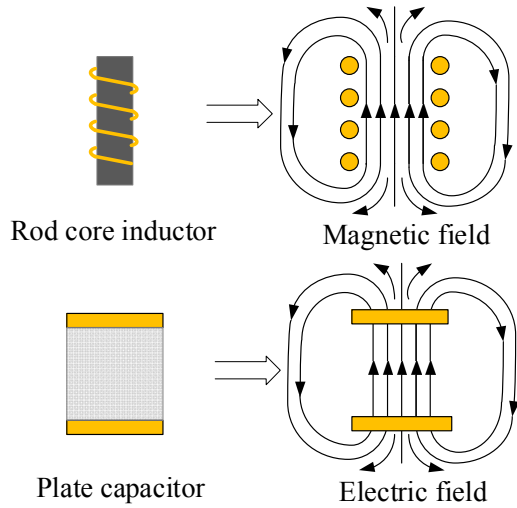


Fig. 1. The analogy between the electric field of plate capacitors and the magnetic field of rod core inductors.

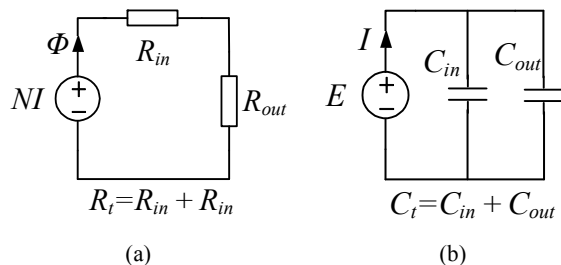


Fig. 2. The duality between (a). magnetic circuits and (b). electrical circuits.

Since the space and material outside winding do not change without the insertion of the rod ferrite core, R_{out_air} and R_{out_f} can be assumed as the same value. However, the reluctance inside winding with rod ferrite core will decrease μ_f times than the one of the air-core inductor because of the high permeability of ferrite material. L_{air} is well studied with previous literature, so the only unknown term in Eq. 1 is the reluctance ratio between inside windings and outside windings for an air-core inductor. To derive the reluctance ratio, an analogy between reluctances and capacitances is applied. As shown in Fig. 1, the magnetic fields of rod core

inductors and the electric fields of plate capacitors are quite similar. Also, based on the duality of reluctance and capacitance from Fig. 2 and Eq. 2, the reluctance can be analogized to the reciprocal of the capacitance. Hence, the reluctance ratio between inside and outside windings is converted to a derivation of the capacitance ratio between outside and inside plates, shown as Eq. 2.

$$\left. \begin{aligned} R &= \frac{1}{\mu_0 \mu_r} \frac{l}{A} \\ C &= \epsilon_0 \epsilon_r \frac{A}{l} \end{aligned} \right\} \Rightarrow R \sim \frac{1}{C} \Rightarrow \frac{R_{in_air}}{R_{out_air}} = \frac{C_{out}}{C_{in}} \quad (2)$$

The reason for using the analogy is the external magnetic fields outside winding is more complex and less well known, while the electric fields of such a structure in Fig. 1 is provided by Austin [7] for a monopole antenna. Then the reluctance ratio is obtained from the capacitance ratio in Eq.3.

$$\frac{R_{in_air}}{R_{out_air}} = \frac{C_{out}}{C_{in}} \approx \frac{l_c}{\pi r_c^2} / \frac{1}{3.49 r_c} \quad (3)$$

$$= \frac{3.49 l_c}{\pi r_c} \approx 1.022 \frac{l_c}{r_c}$$

where l_c is the length of the winding coil, and the r_c is the radius of the winding coil.

With the reluctance ratio, the final closed-form equation of the rod core inductance can refer to paper [6], and Payne [6] claims that the error of the proposed rod core inductance model is within 1.5%. To validate the effectiveness of using Payne's model to predict leakage inductance of CM choke, a ferrite toroidal core ZW435610TC from Magnetics was used to build CM chokes with different turns numbers. The comparison results with Nave's model and measuring results are shown in Fig. 3. As shown in Fig. 3, with few turns number, both Payne's model and Nave's model achieve high accuracy. Nonetheless, when turns number increases from 7 to 28, the error of Nave's model increases from 7.4% to 36.6% and the error of Payne's model also increases from 1.67% to 26.86%.

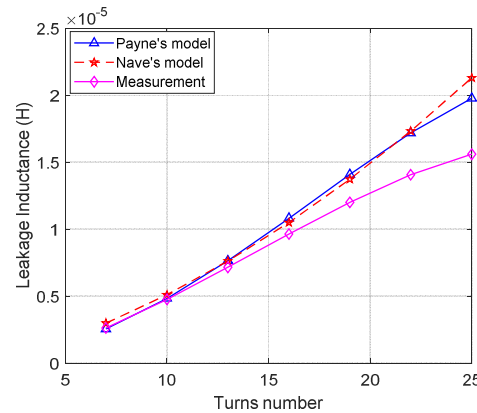


Fig. 3. Leakage modeling comparison with two models.

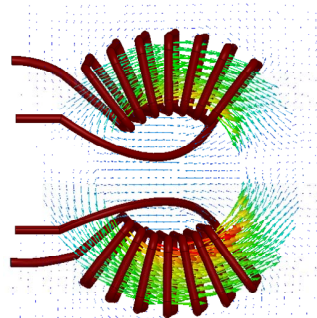
From the above analysis, although Payne's rod core inductance model achieves a smaller error compared to the Nave's leakage model, the error is still large when the winding has many turns.

III. LEAKAGE INDUCTANCE OF CM CHOKE DERIVATION

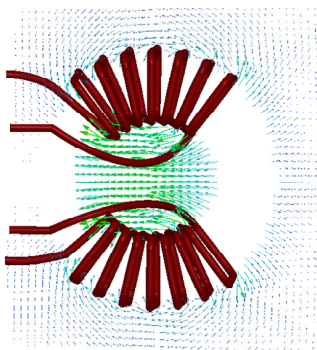
Only using the rod core inductance model is not accurate enough for the leakage evaluation for the toroidal CM choke especially when the turns number is large. Fig. 4(a) illustrates the magnetic fields of a two-phase CM choke for both DM and CM flux and Fig 4(b) displays only the leakage flux distribution. As can be seen, the leakage flux distribution in Fig. 4(b) is obviously different from the magnetic fields of rod core inductor. For the upper winding, the fluxes outside winding are not symmetrical and the amplitude of fluxes in the lower side of the winding is obviously larger than that in the upper side of winding. Hence, the assumption for Eq. 1 that R_{out_air} and R_{out_f} have the same value is not correct since the distribution of leakage flux with the large turns number has been changed. Eq. 1 for leakage inductance derivation must be corrected as

$$L_f = L_{air} (L_f / L_{air}) = \frac{R_{in_air} + R_{out_air}}{R_{in_f} + R_{out_f}} L_{air} \quad (4)$$

$$= \frac{R_{in_air} / R_{out_air} + 1}{(R_{in_air} / \mu_f) / R_{out_air} + R_{out_f} / R_{out_air}} L_{air}$$



(a) Both CM and DM flux



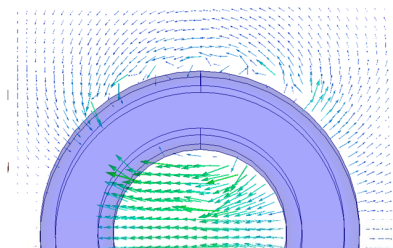
(b) Only DM (leakage) flux

Fig. 4. Magnetic fields of two-phase CM choke (hiding toroidal core)

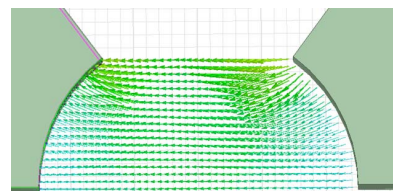
Compared with Eq. 1, Eq. 4 needs to derive R_{out_f} over R_{out_air} . The solution here is still to convert the derivation of the reluctance ratio to the derivation of the capacitance ratio. To construct the electric field analogy for the magnetic fields of leakage flux of the CM choke with a large turns number, a new geometry of metal sheet is given in Fig. 5(b). Comparing Fig. 5(a) and 5(b), the leakage flux inside the toroidal core is close to the electric field of the two curved metal surfaces. With this the analogy assumption, the reluctance ratio of R_{out_f} over R_{out_air} can be derived as Eq. 5 by the calculation of the capacitance of two curved surfaces.

$$\frac{R_{out_f}}{R_{out_air}} = \frac{C_{out_air}}{C_{curved} + C_{out_air} / 2} \quad (5)$$

where C_{curved} is the capacitance of two curved surfaces.



(a) Leakage flux distribution



(b) Electric fields of two curved surfaces

Fig. 5. The analogy of magnetic fields and electric fields for a CM choke with a large turns number.

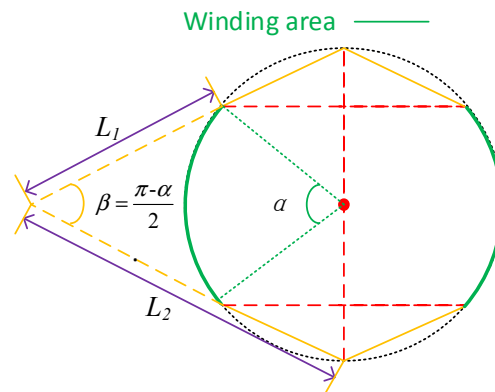


Fig. 6. Geometry equivalent transformation from curved faces to folded planes.

To simplify the derivation of C_{curved} , two curved faces are regarded as two folded planes shown in Fig. 6 with the solid orange curves. With this equivalent geometry, the derivation of the capacitance of two curved faces is converted into the

derivation of the capacitance of two non-parallel planes shown in Fig. 7.

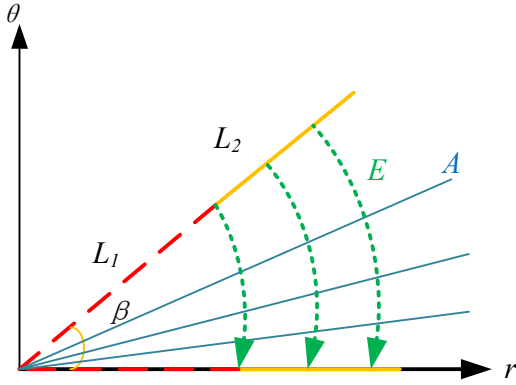


Fig. 7. Electric field for non-parallel planes in polar coordinates.

Based on the symmetry, any plane including the origin point is the equipotential plane for the electric field inside two non-parallel planes. As a result, the electric field intensity is only related to the distance r from the origin point and the direction of the electric field is perpendicular to equipotential planes. With this observation, electric field intensity and electrical potential inside two planes are written as

$$\begin{aligned} E_{(r,\theta)} &= E_r e_\theta \\ U_{(r,\theta)} &= U_\theta \end{aligned} \quad (6)$$

Due to the continuity of potential, the electrical potential in polar coordinate can be analyzed as

$$\frac{\partial^2 U}{\partial r^2} + \frac{1}{r} \frac{\partial U}{\partial r} + \frac{1}{r^2} \frac{\partial^2 U}{\partial \theta^2} = 0 \quad (7)$$

From Eq. 6, the electrical potential is irrelevant to the distance r , so Eq. 7 is simplified as

$$\frac{1}{r^2} \frac{\partial^2 U}{\partial \theta^2} = 0 \quad (8)$$

Eq. 8 can be solved with the general solution of a quadratic differential equation with the initial conditions:

$$U = U_1 - \frac{U_1 - U_2}{\beta} \theta \quad (9)$$

$$\text{where } \theta = 0, U = U_1; \theta = \beta, U = U_2$$

Then, the electric field intensity and charge density can be derived as

$$\begin{cases} E = -\nabla U = \frac{U_1 - U_2}{ra} \\ \sigma_r = \epsilon_0 E = \frac{U_1 - U_2}{ra} \epsilon_0 \end{cases} \quad (10)$$

The capacitance of non-parallel planes finally is calculated based on the definition:

$$\begin{aligned} C &= \frac{Q}{\Delta U} = \frac{\int_{L_1}^{L_2} \sigma_r dS}{U_1 - U_2} \\ &= \frac{H_t \epsilon_0 \frac{U_1 - U_2}{\beta} \int_{L_1}^{L_2} \frac{1}{r} dr}{U_1 - U_2} = \frac{H_t \epsilon_0}{\beta} \ln \frac{L_2}{L_1} \end{aligned} \quad (11)$$

where L_1 and L_2 are labeled in Fig. 6, β is the angle between two non-parallel planes, α is the winding angle, H_t is the height of the core.

Substituting L_2 and L_1 by the calculations with the dimensions of the core, C_{curved} is obtained as

$$\begin{aligned} C_{curved} &= \frac{2H_t \epsilon_0}{\beta} \ln \frac{r_{inner} / \sin(\beta/2)}{r_{inner} \cos(\beta) / \sin(\beta/2)} \\ &= \frac{2H_t \epsilon_0}{\beta} \ln \frac{1}{\cos(\beta)} \end{aligned} \quad (12)$$

where r_{inner} is the radius of the inner side of the core.

The second approach to estimate the capacitance of two curved faces is to directly apply the equation for the capacitance of parallel plates since the electric field between two curved faces shown in Fig. 5(b) is very similar to the electric field of two parallel plates. The surface area is approximated with using the curved face's area, and the distance between two curved faces is averaged by the maximum and the minimum values. The final expression is:

$$\begin{aligned} C_{curved_sc} &= \frac{\epsilon_0 (\pi - \alpha) H_t r_{inner}}{(2r_{inner} + 2r_{inner} \cos(\beta)) / 2} \\ &= \frac{\epsilon_0 (\pi - \alpha) H_t}{1 + \cos(\beta)} \end{aligned} \quad (13)$$

Combining Eq. 3, Eq. 4, and Eq. 12 or Eq. 13, the corrected leakage inductance can be calculated.

For the first proposed model, C_{curved} is derived by the equivalent geometry and the capacitance of non-parallel plates. The reluctance ratio of R_{out_f} over R_{out_air} is:

$$\left. \frac{R_{out_f}}{R_{out_air}} \right|_{first} = \frac{3.49r_c}{\frac{2H_t \epsilon_0}{\beta} \ln \frac{1}{\cos(\beta)} + 3.49r_c / 2} \quad (14)$$

For the second proposed model, C_{curved} is derived by the approximation of curved faces as the two parallel plates. The reluctance ratio of R_{out_f} over R_{out_air} is:

$$\left. \frac{R_{out_f}}{R_{out_air}} \right|_{second} = \frac{3.49r_c}{\frac{\epsilon_0(\pi - \alpha)H_l}{1 + \cos(\beta)} + 3.49r_c / 2} \quad (15)$$

Two derived models with different expressions of C_{curved} will be compared with Nave's model in the next section. The detailed implementation of the proposed models is given in the Appendix. The source code of the proposed models and adopted simulation data for comparisons are open access in Github.

IV. VERIFICATION OF THE PROPOSED LEAKAGE MODEL

To verify the effectiveness of the proposed model, 3-D FEM simulations were conducted in COMSOL, and the simulation results were provided and verified by the paper [5] and have only a 1% error compared with the measuring results.

Fig. 8 (a)-(d) gives the comparison results for the toroidal ferrite core ZW43610TC with AWG 26 wires and AWG 11wires. As it shows in Fig. 8(b), the errors of the proposed models drop from 40% to 10% compared with Nave's model when the turns number is 55. For different turns numbers, the errors of the proposed model 2 keep within 10%, and errors of proposed model 1 keep within 15%. The proposed model 2 achieves a little bit higher accuracy at 55 turns.

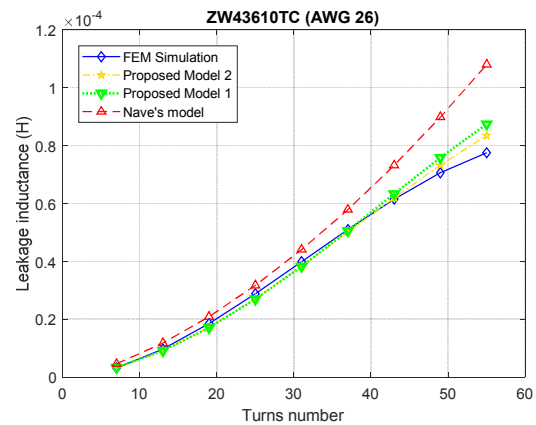
In Fig. 8 (d), when the winding changes to AWG #11 wires, for different turns numbers, the errors of the proposed model 1 and 2 are both below 10%. However, the proposed model 1 can achieve 5% less error compared with the proposed model 2 at 10 turns.

Fig. 9 (a)-(d) shows another example for the toroidal ferrite core ZW44825TC with AWG #20 wires and AWG #8 wires. When using AWG #20 wires, as same as the first case, the maximum error of the proposed model drops from 40% to 5% compared with Nave's model when the turns number is 20. However, in this case, when the turns number is 5, Nave's model shows better accuracy. For other turns number except 5, the proposed models show much better accuracy.

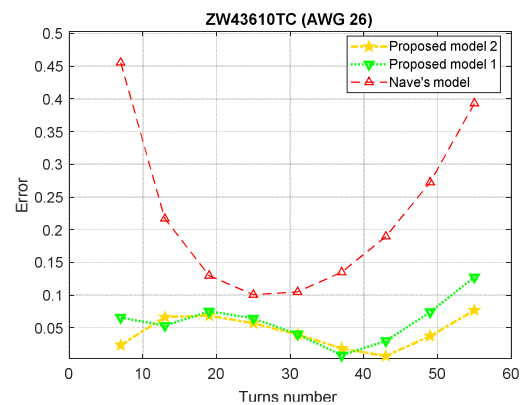
In Fig. 9 (d), when the winding changes to AWG #8 wires, for different turns numbers, the errors of the proposed model 1 and 2 are both below 5%. In the whole turns number range, the proposed models show a much higher accuracy. In addition, the proposed model 1 has 3% less error compared with the proposed model 2.

From comparisons, the proposed models show a much higher accuracy in most cases, especially for the large turns number. Only at two testing points with the low turns number, Nave's model has better accuracy, but the proposed models also have acceptable accuracy within 15% at those points. The proposed model 1 has better accuracy when using a larger wire diameter compared with the proposed model 2. For wires with smaller wire diameter, the proposed model 2 shows better accuracy than the proposed model 2. But in general, two proposed models both can achieve much

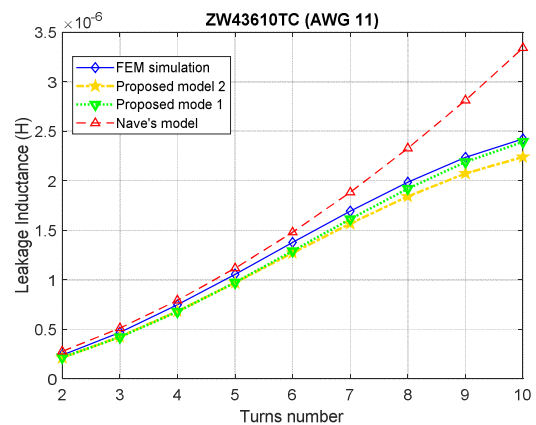
higher accuracy compared with Nave's model, and the errors in different cases are lower than 15%.



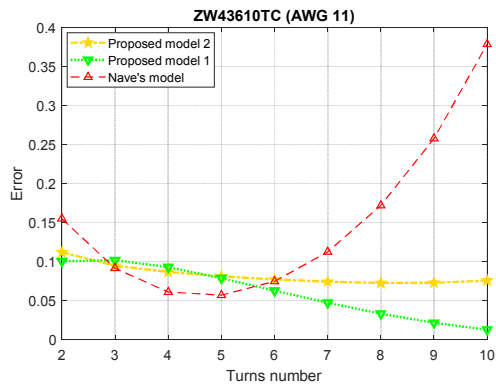
(a) Leakage inductance comparison with AWG #26 winding



(b) Absolute error comparison with AWG #26 winding

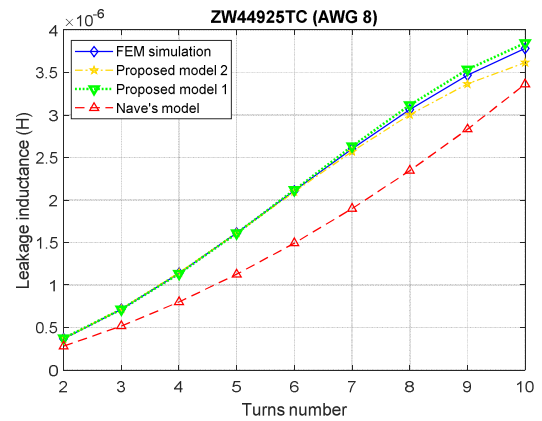


(c) Leakage inductance comparison with AWG #11 winding

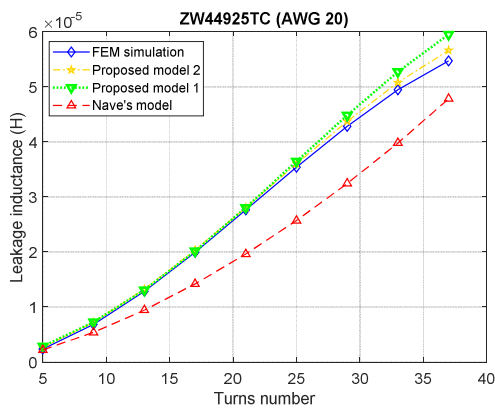


(d) Absolute error comparison with AWG # 11 winding

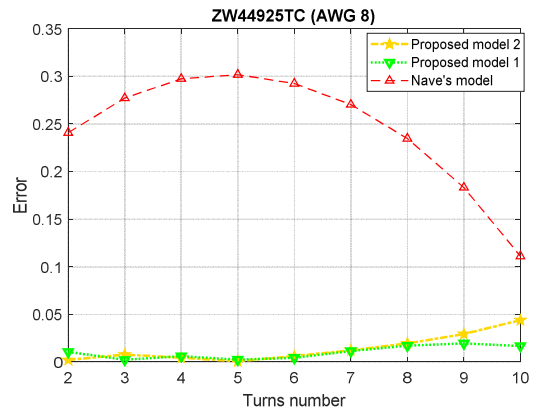
Fig. 8. Comparison of leakage inductance models with FEM simulation results for magnetic core ZW43610TC.



(c) Leakage inductance comparison with AWG #8 winding

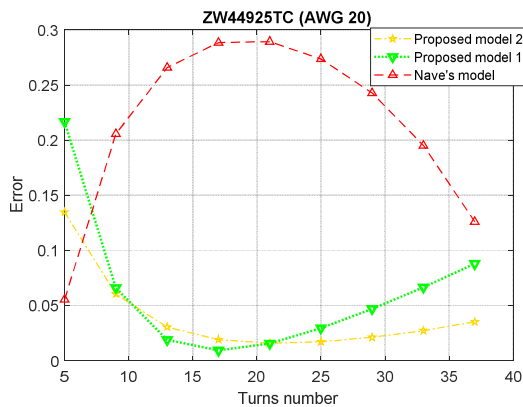


(a) Leakage inductance comparison with AWG #20 winding



(d) Absolute error comparison with AWG # 8 winding

Fig. 9. Comparison of leakage inductance models with FEM simulation results for magnetic core ZW44925TC.



(b) Absolute error comparison with AWG # 20 winding

V. CONCLUSIONS

Nave's model cannot predict the leakage inductance accurately at large turns number. From the perspective of the analogy between reluctances and capacitances, this paper proposes a leakage inductance model to improve accuracy when the CM choke has a large turns number. Two models are developed based on the different ways to derive the capacitance of two curved faces. The 3D FEM simulation verifies the proposed model can reduce 25%~30% errors compared with Nave's model at large turns number. In addition, the proposed model with a simple form is easy to implement compared with the integral form of formulae in [1].

ACKNOWLEDGMENT

This work was supported primarily by the Engineering Research Center Program of the National Science Foundation and the Department of Energy under NSF Award Number EEC1041877 and the CURENT Industry Partnership Program.

APPENDIX

An air core inductance derivation from capacitance is given in reference [6]. Here gives the procedure to illustrate how to do the calculation.

$$\begin{aligned}
 l_c &= l_e \cdot \frac{\alpha}{2\pi} \\
 l_f &= l_e / 2 \\
 l_{c1} &= l_c + 0.45d_c \\
 x &= \frac{R_{in_air}}{R_{out_air}} = \frac{5.1 \cdot (l_{c1} / d_c)}{(1 + 2.8(d_c / l_{c1}))} \\
 l_{fc1} &= l_f - l_c \\
 \mu_{fe} &= (\mu_f - 1)(d_f / d_c)^2 + 1 \\
 K_n &= \frac{1}{(1 + 0.45(d_c / l_c) - 0.005(d_c / l_c)^2)} \\
 A &= (d_c / 2)^2 \pi \\
 L_{air} &= \frac{\mu_0 \cdot N^2 \cdot A \cdot K_n}{l_c}
 \end{aligned} \tag{A.1}$$

where l_e is the effective magnetic flux path length of the core, l_c is the winding covered path length, d_f and d_c are the diameters of the core and coil, μ_f is the relative permeability of the core material, μ_0 and ϵ_0 are the vacuum permeability and dielectric permittivity. Other parameters do not have physical meaning and are only used as intermediate variables for calculations.

With the derived air inductance, the proposed leakage inductance can be derived as

$$\begin{aligned}
 k &= \frac{R_{out_f}}{R_{out_air}} \Bigg|_{first} = \frac{1.75 \cdot d_f}{\frac{2H_t \epsilon_0}{\beta} \ln \frac{1}{\cos(\beta)} + 1.75 \frac{d_f}{2}} \\
 \text{or } k &= \frac{R_{out_f}}{R_{out_air}} \Bigg|_{second} = \frac{1.75 \cdot d_f}{\frac{\epsilon_0 (\pi - \alpha) H_t}{1 + \cos(\beta)} + 1.75 \frac{d_f}{2}} \\
 L_{lk} &= \frac{1 + x}{(k + x / \mu_{fe})} L_{air}
 \end{aligned} \tag{A.2}$$

The open-source code and testing data are provided by the following link:

https://github.com/Potato-Ren/Leakage_Inductance_Model

REFERENCES

[1] D. J. Wilcox, M. Conlon, and W. G. Hurley, "Calculation of self and mutual impedances for coils on ferromagnetic cores," in *IEE Proceedings A - Physical Science, Measurement and*

Instrumentation, Management and Education - Reviews, vol. 135, no. 7, pp. 470-476, September 1988

[2] I. Hernandez, F. de Leon and P. Gomez, "Design Formulas for the Leakage Inductance of Toroidal Distribution Transformers," in *IEEE Transactions on Power Delivery*, vol. 26, no. 4, pp. 2197-2204, Oct. 2011.

[3] M. J. Nave, "On modeling the common mode inductor," *IEEE 1991 International Symposium on Electromagnetic Compatibility*, Cherry Hill, NJ, USA, 1991, pp. 452-457.

[4] M. L. Heldwein, L. Dalessandro, and J. W. Kolar, "The Three-Phase Common-Mode Inductor: Modeling and Design Issues," *IEEE Trans. Ind. Electron.*, vol. 58, no. 8, pp. 3264-3274, 2011.

[5] Zhou Dong, Ren Ren, Bo Liu, Fred Wang, "Data-driven leakage inductance modeling of common mode chokes," *2019 IEEE Energy Conversion Congress and Exposition (ECCE)*, Baltimore, MD, 2019.

[6] PAYNE A N. 'The Inductance of a Single Layer Coil derived from Capacitance', <http://g3rbj.co.uk/>

[7] Morecraft, J. H. (1927). Principles of radio communication, 1927.